Structure Design and Kinematic Analysis of a Partially-Decoupled 3T1R Parallel Manipulator

Ke Xu[1], Haitao Liu[1](✉), Huiping Shen[2], and Tingli Yang[2]

[1] Key Laboratory of Mechanism Theory and Equipment Design, Ministry of Education, Tianjin University, Tianjin 300350, China
liuht@tju.edu.cn

[2] School of Mechanical Engineering, Changzhou University, Changzhou 213016, China

Abstract. A partially-decoupled three-translation and one-rotation (3T1R) parallel manipulator is proposed and analyzed in this paper. The new mechanism features with a symmetric layout and simple kinematic structure for generation of 3T1R motion in pick-and-place operations. The kinematics of this mechanism, including forward and inverse position problems, are analyzed. The closed-form solution of direct kinematics is obtained and verified by inverse kinematics. Moreover, the partially-decoupled performance can be found through the forward kinematics. The proposed mechanism is mainly composed of revolute joints and presents better performance. Hence, more potential applications of this manipulator can be expected.

Keywords: 3T1R · Parallel mechanism · Structure design · Kinematic analysis

1 Introduction

The parallel manipulators (PMs) with three translations and one rotation (3T1R), also known as Schönflies-motion parallel robots, have a great potential of various applications in the manufacturing industry. Many 3T1R robots have been proposed and developed. Examples include H4 [1], I4 [2], I4R [3], Par4 [4], Heli4 [5]. These robots have similar architectures but with different designs of the moving platform. A parallel Schönflies-motion robot admitting a rectangular workspace, which allows to utilize the shop-floor space efficiently for flexible pick-and-place applications, was recently proposed by Wu et al. [6]. Many other 3T1R robots constructed adopting quite different kinematic structures are available in literature. Zhao, Huang et al. [7] proposed a 4-URU-type 3T1R parallel robot. Jin and Yang [8] proposed a family of 3T1R parallel mechanisms based on single-open-chain structures. Kong et al. [9] synthesized a group of PMs with the same sub-chains based on screw theory. Huang et al. [10] developed a 3T1R-type high-speed parallel manipulator called as Cross-IV. Liu et al. [11] developed a X4 parallel robot prototype with one moving platform.

It is noted that the above stated 3T1R parallel mechanisms all have higher coupling degree, and are not input-output motion decoupled, which lead to their forward

H. Yu et al. (Eds.): ICIRA 2019, LNAI 11742, pp. 415–424, 2019.
https://doi.org/10.1007/978-3-030-27535-8_37

kinematics and dynamics analysis, motion control and trajectory planning are more complex. Partially or fully decoupled parallel manipulators are desirable. There are already some parallel mechanisms with partial motion decoupling or complete decoupling properties proposed, for example, mechanisms of decoupled two-rotation DOF [12], one-translation and two-rotation DOF [13], three-translation [14], etc. Examples include also a XYZ parallel elasticity mechanism [15], a partially decoupled 3-PPR robot with U-shape base [16]. In spite of the above proposed partially decoupled parallel mechanisms, very few 3T1R PMs with motion decoupling are reported. The SCARA parallel robot of FlexPicker [17] has partial motion decoupling, which is based on the Delta mechanism, attached with a RUPU kinematic chain, in order to achieve the rotation around the normal of the moving platform.

In this paper, a novel partially-decoupled 3T1R parallel manipulator is proposed. The kinematics analysis of this 3T1R PM is also the subject of this paper. The paper is organized as follows: Sect. 2 illustrates this 3T1R PM of 2-(RPa||3R)3R with type synthesis method based on POC equations [18]. In Sect. 3, the closed-form equations are established and the direct kinematics of this mechanism is solved. The reported work is concluded in Sect. 4.

2 Structure Design of a 2-(RPa||3R)3R Manipulator

The 3T1R parallel manipulator proposed here is shown in Fig. 1. The base platform 0 is connected to the moving platform 1 by left and right two identical hybrid chains. Each hybrid chain contains a sub-parallel mechanism (sub-PM) and a 3R serial kinematic chain. The manipulator is symmetrical about the plane $x-y=0$. The intersecting line of the plane and the base is the line *t*-*t*.

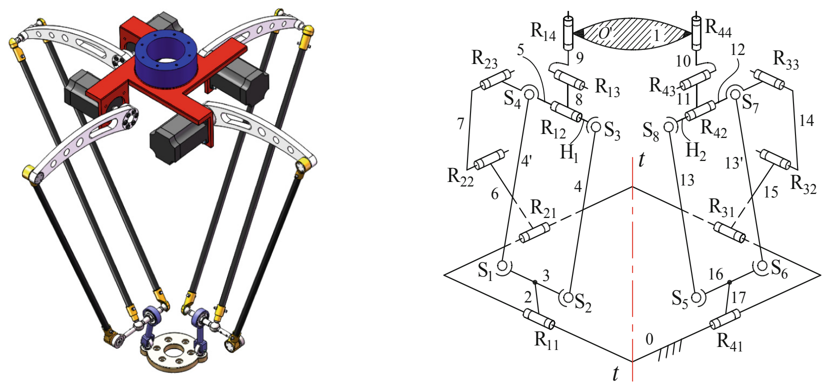

(a) 3D CAD model (b) Kinematic structure

Fig. 1. 3D CAD model and kinematic structure of 3T1R robot

With reference to the symmetric plane, the left hybrid chain composed of links 2, 3, 4, 4′, 5, 6, 7, 8 and 9, as shown in Fig. 1(b), is selected to illustrate the structure of manipulator. The CAD design of the hybrid chain is shown in Fig. 2(a). The shorter link 3 of a parallelogram composed of four spherical pairs (S_1, S_2, S_3 and S_4) is connected by actuated arm 2, to the base 0 by a revolute joint R_{11}, which is denoted as RPa. The extended part of the opposite link 5 of the parallelogram is connected in parallel to a sub-chain composed of two links 6 and 7 and three parallel revolute joints (3R, i.e., $R_{21}\|R_{22}\|R_{23}$). The connection line of the two spherical joints S_3 and S_4 is collinear with the axis of the rotation joints R_{12} but perpendicular to the axis of the revolute joint R_{23}. Thus, a sub-parallel mechanism (sub-PM) is generated, as shown in Fig. 2(b), and denoted as RPa‖3R.

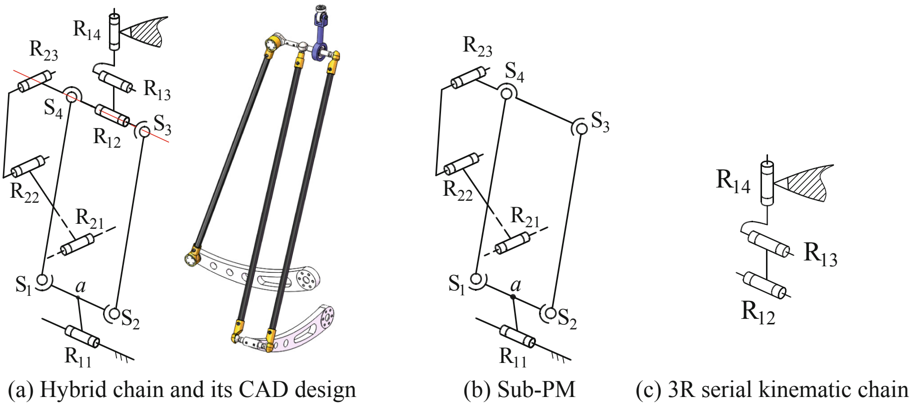

Fig. 2. Kinematic structures of chains

This sub-PM is then further connected with a 3R serial kinematic chain composed of two links 8 and 9 and 3R serial kinematic chain, i.e., $R_{12}\|R_{13}\perp R_{14}$, as shown in Fig. 2(c), which leads to a hybrid chain. Since the PM has two identical hybrid chains, the whole manipulator is recorded as 2-(RPa‖3R)3R. The four rotation joints R_{11}, R_{21}, R_{31} and R_{41} on the base platform 0 are active and mutually perpendicular to each other, which means $R_{11}\perp R_{41}$, $R_{11}\perp R_{21}$ and $R_{41}\perp R_{31}$. Two rotation joints R_{14} and R_{44} on the moving platform are all parallel to the normal of the moving platform 1, i.e., $R_{14}\|R_{44}$. Here, the symbols ‖ and ⊥ stand respectively for being parallel and vertical, the same hereinafter.

3 Kinematic Analysis

3.1 Establishment of the Coordinate System and Parameterization

Without losing of generality, let the base platform 0 be a square. The four actuated joints R_{11}, R_{21}, R_{31} and R_{41} are located on the midpoint of its each side, i.e., A_1, A_2, A_3, A_4, as shown in Fig. 3. Furthermore, the frame coordinate system *o-xyz* is established on the base platform 0. The origin is located at the geometric center, point *o*, of the base platform 0. The axes *x* and *y* are collinear with and vertical to the connection line $\boldsymbol{A}_1\boldsymbol{A}_3$, respectively. On the moving platform 1, the moving coordinate system *p*-*uvw* is established at point *p* that is the midpoint of the connection line between the points F_1 and F_2. *u* axis is perpendicular to the line $\boldsymbol{F}_1\boldsymbol{F}_2$, while *v* axis coincides with this line $\boldsymbol{F}_1\boldsymbol{F}_2$. Both *z* and w axes are determined by the right-hand Cartesian coordinate rule, as shown in Fig. 3(a). For ease of understanding, the 2-(RPa||3R)3R PM is redrawn as stretched to a planar view, as shown in Fig. 3(b).

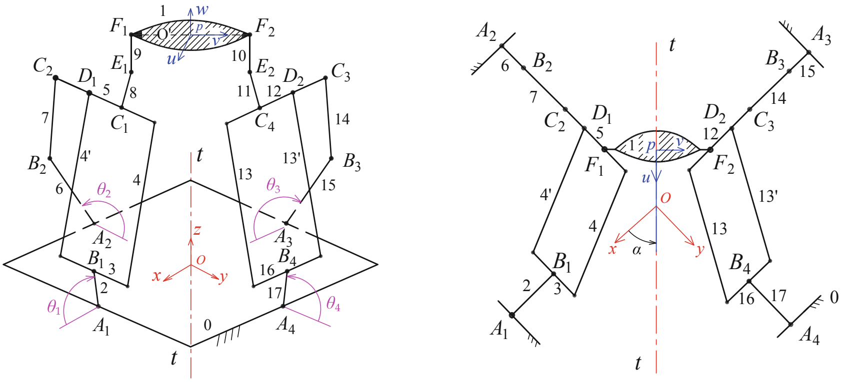

(a) The structure parameters of this PM (b) Expansion of the kinematic chain

Fig. 3. Parameterizations of the 2-(RPa||3R)3R PM

The structure parameters of the PM are denoted in the following way. The side length of the square base platform 0 is noted by $2l_1$, and the length of the moving platform 1, i.e., $F_1F_2 = 2l_2$. For other link lengths, we have

$$A_1B_1 = A_2B_2 = A_3B_3 = A_4B_4 = l_3(l_3 \neq l_1),\ B_1C_1 = B_2C_2 = B_3C_3 = B_4C_4 = l_4$$
$$D_1C_1 = C_2D_1 = C_3D_2 = C_4D_2 = l_5,\ C_1E_1 = C_4E_2 = F_1E_1 = F_2E_2 = l_6$$

The four input angles are defined as θ_1, θ_2, θ_3 and θ_4 for the four active joints, as shown in Fig. 3(a). The moving platform position is defined by the coordinates of point *p* as (*x*, *y*, *z*), and its orientation by angle α, the angle from the forward direction of *u*-axis to *x*-axis or from the forward direction of *v*-axis to *y*-axis, as shown in Fig. 3(b).

3.2 Solution to Forward Position Problem

In the forward position analysis, we need to obtain output parameters, i.e., the coordinates of point *p* of the moving platform, defined by (*x*, *y*, *z*), and the orientation angle α, as a function of the known input angles θ_1, θ_2, θ_3 and θ_4.

Solve Coordinates of Points C_1 and C_4. The coordinates of four points A_1, A_2, A_3 and A_4 on the base platform 1 are $(l_1,0,0)$, $(0,-l_1,0)$, $(-l_1,0,0)$ and $(0,l_1,0)$, respectively. The coordinates of each end point of the four actuated arms 2, 6, 15 and 17, i.e., points B_1, B_2, B_3 and B_4, are easily calculated as respectively, $(l_1 + l_3\cos\theta_1,0,\ l_3\sin\theta_1)$, (0,$-l_1$ + $l_3\cos\theta_2$, $l_3\sin\theta_2$), ($-l_1$ + $l_3\cos\theta_3$,0, $l_3\sin\theta_3$) and (0, l_1 + $l_3\cos\theta_4$, $l_3\sin\theta_4$). As stated in Sect. 2.2.1, the output links 5 and 12 of the left and right sub-PMs can only produce a motion in the plane *o-yz* and *o-xz* respectively. That is, $x_{C1} = 0$ and $y_{C4} = 0$. Hence, the coordinates of points C_2 and C_3 are found as $(0, y_{C1} - 2l_5, z_{C1})$ and $(x_{C4} - 2l_5, 0, z_{C4})$ respectively. The link length constraints defined by $B_1C_1 = B_2C_2 = B_3C_3 = B_4C_4 = l_4$ imply that

$$\begin{cases} x_{B_1}^2 + y_{C_1}^2 + (z_{B_1} - z_{C_1})^2 = l_4^2 \\ (y_{B_2} - y_{C_1} + 2l_5)^2 + (z_{B_2} - z_{C_1})^2 = l_4^2 \end{cases} \quad (1)$$

$$\begin{cases} x_{C_4}^2 + y_{B_4}^2 + (z_{B_4} - z_{C_4})^2 = l_4^2 \\ (x_{B_3} - x_{C_4} + 2l_5)^2 + (z_{B_3} - z_{C_4})^2 = l_4^2 \end{cases} \quad (2)$$

Equation (1) leads to

$$a_1 y_{C_1} + b_1 z_{C_1} = c_1 \quad (3)$$

here, $a_1 = 2(y_{B2} + 2l_5), b_1 = 2(z_{B2} - z_{B1}),\quad c_1 = (y_{B2} + 2l_5)^2 + z_{B2}^2 - x_{B1}^2 - z_{B1}^2$. If $a_1 = 0$ and $b_1 = 0$, then $c_1 = -x_{B1}^2 = 0$. However, due to $l_3 \neq l_1$, i.e., $x_{B1} \neq 0$, a_1 and b_1 are not zero at the same time. Hence, we have two cases as follows

$$\begin{cases} z_{C_1} = \frac{c_1}{b_1}, y_{C_1} = \pm\sqrt{l_4^2 - (z_{B_1} - z_{C_1})^2 - x_{B_1}^2} \; if \; a_1 = 0 \\ z_{C_1} = \frac{e_1 \pm \sqrt{e_1^2 - 4d_1 f_1}}{2d_1}, y_{C_1} = \frac{c_1 - b_1 z_{C_1}}{a_1} \; if \; a_1 \neq 0 \end{cases} \quad (4)$$

here, $d_1 = a_1^2 + b_1^2,\quad e_1 = 2(b_1 c_1 + z_{B1} a_1^2),\quad f_1 = a_1^2(x_{B1}^2 + z_{B1}^2 - l_4^2) + c_1^2$. Similarly, Eq. (2) leads to $a_2 x_{C4} + b_2 z_{C4} = c_2$ and coordinates of point C_4 can be obtained.

Solve Coordinates of Point *p* and Orientation *α*. Once the coordinates of points C_1 and C_4 are obtained, the upper parts of each hybrid chain, i.e., links 8, 9 and 10, 11, and the moving platform 1 can be treated as a special single loop chain 6R mechanism, as shown in Fig. 4(a). A planar view is shown in Fig. 4(b).

As shown in Fig. 4(a), let δ be the angle between vector $\boldsymbol{C_1E_1}$ and *x*-axis. We assume two planes *m* and *n* pass through the points C_1, E_1 and F_1, and the points C_4, E_2 and F_2, respectively, as shown in Fig. 4(b). Thus, motions of two groups of points (C_1, E_1, F_1) and (C_4, E_2, F_2) always keep in the planes *m* and *n*, respectively. Then, we get

$$y_{E_1} = y_{C_1}, x_{E_2} = x_{C_4} \quad (5)$$

Hence the coordinates of points E_1 and E_2 are calculated. The constraint equation is expressed as $y_{E2}^2 + (z_{C4} - z_{E2})^2 = l_6^2$. It is obtained, due to $z_{E1} = z_{E2}$ and $y_{C4} = 0$, by

$$y_{E_2} = \pm\sqrt{l_6^2 - (z_{C_4} - z_{C_1} - l_6 \sin\delta)^2} \quad (6)$$

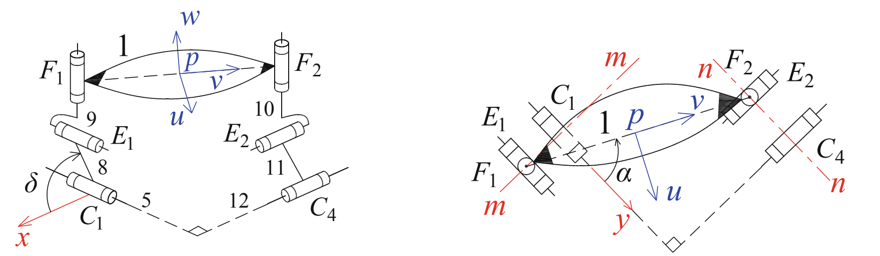

(a) Single loop space 6R mechanism (b) Plan view of single loop 6R mechanism

Fig. 4. Upper part of the robot

From Fig. 3(b), it is known that $F_1F_2 = E_1E_2 = 2l_2$, and hence we establish another constraint equation as

$$(x_{C_4} - l_6\cos\delta)^2 + (y_{E_2} - y_{C_1})^2 = 4l_2^2 \tag{7}$$

Let $u = \tan\delta/2$. By expanding Eq. (7), we obtain a high-order polynomial equation with only one variable u as following

$$f(u) = \sum_{i=0}^{8} g_i u^i \tag{8}$$

$$\begin{aligned}
g_0 = {} & 16l_2^4 - 16l_2^2l_6^2 + 4l_6^4 + 8l_2^2t^2 - 4l_6^2t^2 + t^4 + x_{C_4}(16l_2^2l_6 - 8l_6^3 + 4l_6t^2 - 8l_2^2x_{C_4} \\
& + 8l_6^2x_{C_4} - 2t^2x_{C_4} - 4l_6x_{C_4}^2 + x_{C_4}^3) - y_{C_1}^2(8l_2^2 - 2t^2 + 4l_6x_{C_4} - 2x_{C_4}^2 - y_{C_1}^2), \\
g_1 = {} & 8l_6t(2l_6^2 - 4l_2^2l_6 - 2l_6t^2 - 2l_6x_{C_4} + l_6x_{C_4}^2 - l_6y_{C_1}^2), \\
g_2 = {} & 4(16l_2^4 - 4l_6^4 + 8l_2^2t^2 + 4l_6^2t^2 + t^4) + 4x_{C_4}(8l_2^2l_6 + 4l_6^3 + 2l_6t^2 - 8l_2^2x_{C_4} - 2t^2x_{C_4} \\
& - 2l_6x_{C_4}^2 + x_{C_4}^3) + 4y_{C_1}^2(2t^2 - 8l_2^2 - 2l_6x_{C_4} + 2x_{C_4}^2 + y_{C_1}^2), \\
g_3 = {} & 8l_6t(3x_{C_4}^2 - 12l_2^2 - 2l_6^2 - 2l_6x_{C_4} - 3y_{C_1}^2 - 3t^2), \\
g_4 = {} & 96l_2^4 + 32l_2^2l_6^2 + 24l_6^4 + 48l_2^2t^2 + 40l_6^2t^2 + 6t^4 - 2x_{C_4}^2(24l_2^2 - 8l_6^2 + 6t^2 + 3x_{C_4}^2) \\
& + 6y_{C_1}^2(2t^2 + 6x_{C_4}^2 - 8l_2^2 + y_{C_1}^2), \\
g_5 = {} & 8l_6t(2l_6x_{C_4} - 12l_2^2 - 2l_6^2 + 3x_{C_4}^2 - 3t^2 - 3y_{C_1}^2), \\
g_6 = {} & 64l_2^4 - 16l_6^4 + 32l_2^2t^2 + 16l_6^2t^2 + 4t^4 - 4x_{C_4}(8l_2^2l_6 + 4l_6^3 + 4l_6t^2 + 8l_2^2x_{C_4} \\
& + 2t^2x_{C_4} + 2l_6x_{C_4}^2 + x_{C_4}^3) + 4y_{C_1}^2(2t^2 - 8l_2^2 + 2l_6x_{C_4} + 2x_{C_4}^2 + y_{C_1}^2), \\
g_7 = {} & 8l_6t(2l_6^2 - 4l_2^2 + 2l_6x_{C_4} + x_{C_4}^2 - y_{C_1}^2 - t^2), \\
g_8 = {} & 4(4l_2^4 - 4l_2^2l_6^2 + l_6^4 + 2l_2^2t^2 - l_6^2t^2)^2 + t^4 + x_{C_4}(8l_6^3 - 16l_2^2l_6 - 4l_6t^2 - 8l_2^2x_{C_4} \\
& + 8l_6^2x_{C_4} - 2t^2x_{C_4} + 4l_6x_{C_4}^2 + x_{C_4}^3) + y_{C_1}^2(4l_6x_{C_4} + 2t^2 - 8l_2^2 + 2x_{C_4}^2 + y_{C_1}^2), \\
t = {} & z_{C_4} - z_{C_1}.
\end{aligned}$$

Real roots of the equation yield the corresponding angle δ, then y_{E2} (with two values) by Eq. (6). By putting y_{E2} values into Eq. (7), we obtain the real value of y_{E2} or y_{C4}. Finally, the coordinates (x, y, z) of point p on the moving platform 1 and rotation angle α can be easily obtained. The equations show that the translation motion of point F_1 on the moving platform 1, along y axis, is determined only by the two joints R_{11} and R_{21} (i.e., θ_1 and θ_2), and the translation motion of point F_2 on the moving platform 1, along x axis, only by the two joints R_{31} and R_{41} (i.e., θ_3 and θ_4), while the translation along z axis and orientation angle α are determined by four input angles θ_1, θ_2, θ_3 and θ_4. In this light, we say the PM has partial motion decoupling property.

3.3 Inverse Position Solution

The purpose of the inverse position solutions is to obtain the input angles θ_1, θ_2, θ_3 and θ_4 as a function of the known output variables, i.e., the coordinates of point p of the moving platform 1, defined by (x, y, z), and the orientation angle of the end-effector α. In the moving coordinate system p-uvw, the coordinates of points E_1 and E_2 are (0, $-l_2$, $-l_6$) and (0, l_2, $-l_6$) respectively. Since the coordinates of points B_1, B_2, B_3 and B_4 are known in the forward position problems afore-mentioned, we may establish the four constraint equations below according to the link length constraints and inverse kinematics can be obtained

$$\theta_i = 2\arctan\frac{2l_3 z_i \pm \sqrt{4z_i^2 l_3^2 - h_i t_i}}{h_i}, (i = 1, 2, 3, 4), \tag{9}$$

$$z_1 = z_{C_1},\ z_2 = z_{C_2},\ z_3 = z_{C_3},\ z_4 = z_{C_4}$$

$$h_1 = l_1^2 - 2l_1 l_3 + l_3^2 - l_4^2 + y_{C_1}^2 + z_{C_1}^2$$

$$t_1 = l_1^2 + 2l_1 l_3 + l_3^2 - l_4^2 + y_{C_1}^2 + z_{C_1}^2$$

$$h_2 = l_1^2 + 2l_1 l_3 + l_3^2 - l_4^2 + 2l_1 y_{C_2} + 2l_3 y_{C_2} + y_{C_2}^2 + z_{C_2}^2$$

$$t_2 = l_1^2 - 2l_1 l_3 + l_3^2 - l_4^2 + 2l_1 y_{C_2} - 2l_3 y_{C_2} + y_{C_2}^2 + z_{C_2}^2$$

$$h_3 = l_1^2 - l_4^2 + 2l_1 l_3 + l_3^2 + 2l_1 x_{C_3} + 2l_3 x_{C_3} + x_{C_3}^2 + z_{C_3}^2$$

$$t_3 = l_1^2 - l_4^2 - 2l_1 l_3 + l_3^2 + 2l_1 x_{C_3} - 2l_3 x_{C_3} + x_{C_3}^2 + z_{C_3}^2$$

$$h_4 = l_1^2 + l_3^2 - 2l_1 l_3 - l_4^2 + x_{C_4}^2 + z_{C_4}^2$$

$$t_4 = l_1^2 + l_3^2 + 2l_1 l_3 - l_4^2 + x_{C_4}^2 + z_{C_4}^2$$

It is easy to find that when the coordinates of the point p and orientation angle of the moving platform 1 are known, the input angles θ_1, θ_2, θ_3 and θ_4 have two sets of solutions, and the points C_1 and C_4 have two sets of the coordinate solutions. Hence the number of the inverse solutions is 64(4 × 16), which leads to the PM has totally 64 configurations.

3.4 Verification of Forward and Inverse Kinematics

The structure parameters are l_1 = 300 mm, l_2 = 70 mm, l_3 = 350 mm, l_4 = 800 mm, l_5 = 100 mm and l_6 = 50 mm, respectively. The four input angles θ_1, θ_2, θ_3 and θ_4 take the values of 58.6839°, 150.8342°, 144.9223° and 61.2457°, respectively. Considering the actual configuration of the PM, we take z_{C1}>0 and z_{C4}>0, according to Eqs. (1)–(4), the coordinates of points C_1 and C_4 are obtained, which are (0, –134.5310, 923.2359) and (–99.1480, 0, 947.7786), respectively. We substitute these values into Eq. (8) and obtain

$$f(u) = 10^8 \times (3.75252 - 1.33078u + 4.45452u^2$$
$$-7.90246u^3 + 8.28859u^4 - 9.84914u^5$$
$$+ 2.29185u^6 - 3.27747u^7 - 1.29474u^8) = 0$$

The real roots of above equation are found as: u_1 = −3.71915, u_2 = 0.867349. The forward solutions are obtained and shown in Table 1.

Table 1. Forward position solutions

No	x /mm	y /mm	z /mm	α /°
1	−71.2029	−70.3510	948.1609	23.5291
2	−46.0400	−88.9291	1022.7338	49.3485

Substituting this group of the forward solutions into the inverse solutions Eq. (9), and considering that z_{E1}>z_{C1}, z_{E2}>z_{C4}, the sets of inverse solutions are reduced to 16, one of which is just one of the given inputs, i.e., θ_1 = 58.684°, θ_2 = 150.8342°, θ_3 = 144.9223° and θ_4 = 61.2457°. The values are consistent with the four known input angles, which verifies the forward and inverse solutions.

4 Conclusion

A novel parallel manipulator 2-(RPa||3R)3R generating three-translation and one-rotation output is proposed. In this work, the kinematics analysis of the new PM was conducted. The close-form forward solutions of the PM are obtained and verified by inverse kinematics. In addition, the PM features motion decoupling which can be found through kinematics.

The contributions of this work are the development of the new 3T1R parallel manipulator 2-(RPa||3R)3R and establishment of its kinematics. The proposed manipulator is symmetric in structure and mainly composed of revolute joints. The new design will lead to less material use and lightweight, and consequentially, a reduced manufacturing cost. Hence, more potential applications can be expected.

References

1. Pierrot, F., Company, O.: H4: A New Family of 4-DOF Parallel Robots. In: 1999 IEEE/ASME International Conference on Advanced Intelligent Mechatronics, Atlanta, USA, pp. 508–513 (1999)
2. Krut, S., Company, O., Benoit, M., et al.: I4: a new parallel mechanism for scara motions. 2008 IEEE Int. Conf. Robot. Autom. **2**(2), 1875–1880 (2008)
3. Krut, S., Nabat, V., Company, O., et al.: A high-speed parallel robot for scara motions. 2004 IEEE International Conference on Robotics and Automation, New Orleans, USA, pp. 4109–4115 (2004)
4. Nabat, V., de la O Rodriguez M., Company, O., et al.: Par4: very high speed parallel robot for pick-and-place. In: IEEE/RSJ International Conference on Intelligent Robots and Systems, IEEE Xplore, Edmonton, Canada, pp. 553–558(2005)
5. Lüdinghausen, M.V., Miura, M., Würzler, N.: Heli4: a parallel robot for scara motions with a very compact traveling plate and a symmetrical design. In: The 2006 IEEE/RSJ International Conference on Intelligent Robots and Systems (IROS), Beijing, China, pp. 1656–1661 (2006)
6. Wu, G., Bai, S., Hjørnet, P.: Architecture optimization of a parallel Schönflies-motion robot for pick-and-place applications in a predefined workspace. Mech. Mach. Theory **09**(5), 148–165 (2016)
7. Zhao, T.S., Huang, Z.: Theory and application of selecting actuating components of spatial parallel mechanisms. Chin. J. Mech. Eng. **36**(10), 81–85 (2000)
8. Yang, T., Jin, Q., Liu, A., et al.: Structure synthesis of 4-dof (3-translation and 1-rotation) parallel robot mechanisms based on the units of single-opened- -chain. In: Proceedings of the ASME 2001 Design Engineering Technical Conference and Computers and Information in Engineering Conference, No. DETC2001/DAC-21152 (2001)
9. Kong, X., Gosselin, C.M.: Type synthesis of 3T1R 4-DOF parallel manipulators based on screw theory. Robot. Autom. IEEE Transact. **20**(2), 181–190 (2004)
10. Huang, T., Zhao, X., Mei, J., et al.: A parallel mechanism with three translations and one rotation, China, ZL201220007884.X (2012)
11. Liu, X., Xie, F.: A kind of four degrees of freedom of moving platform parallel mechanism with SCARA exercise, China, 201210435375.1 (2012)
12. Hou, Y., Lu, W., Zeng, Q., et al.: Motion decoupling two rotational degrees of freedom parallel mechanism, China, 201010617042 (2010)
13. Jin, Q., Yang, T.: Synthesis and analysis of a group of 3-degree-offreedom partially decoupled parallel manipulators. J. Mech. Des. **126**, 301–306 (2004)
14. Kong, X., Gosselin, C.M.: A class of 3-DOF translational parallel manipulators with linear input–output equations. In: Proceedings of the Workshop on Fundamental Issues and Future Research Directions for Parallel Mechanisms and Manipulators, Quebec City, Quebec, Canada, pp. 25–32 (2002)
15. Awtar, S., Ustick, J., Sen, S.: An XYZ parallel-kinematic flexure mechanism with geometrically decoupled degrees of freedom. ASME Int. Des. Eng. Tech. Conf. Comput. Inf. Eng. Conf. **5**(1), 119–126 (2011)

16. Bai, S., Caro, S.: Design and analysis of a 3-PPR planar robot with U-shape base. In: International Conference on Advanced Robotics, Munich, Germany (2009)
17. Liao, B.: A large workspace parallel manipulator for high-speed pick-and-place applications. Harbin Institute of Technology (2012)
18. Yang, T., Liu, A., Shen, H., et al.: Topology Design of Robot Mechanisms. Springer, Singapore (2018). https://doi.org/10.1007/978-981-10-5532-4